Effects of increased pCO$_2$ and temperature on the North Atlantic spring bloom. I. The phytoplankton community and biogeochemical response

Yuanyuan Feng[1,8], Clinton E. Hare[1], Karine Leblanc[1,9,10], Julie M. Rose[1,11], Yaohong Zhang[1], Giacomo R. DiTullio[2], Peter A. Lee[2], Steven W. Wilhelm[3], Janet M. Rowe[3,12], Jun Sun[4], Nina Nemcek[5], Celine Gueguen[5,13], Uta Passow[6], Ina Benner[6], Christopher Brown[7], David A. Hutchins[1,8,*]

[1]College of Marine and Earth Studies, University of Delaware, 700 Pilottown Road, Lewes, Delaware 19958, USA

[2]Hollings Marine Laboratory, College of Charleston, 331 Fort Johnson Road, Charleston, South Carolina 29412, USA

[3]Department of Microbiology, University of Tennessee, 1414 West Cumberland Ave, Knoxville, Tennessee 37996, USA

[4]Key Laboratory of Marine Ecology and Environmental Science, Institute of Oceanology, Chinese Academy of Sciences, Qingdao 266071, PR China

[5]Department of Earth and Ocean Science, The University of British Columbia, 6339 Stores Road, Vancouver, British Columbia V6T 1Z4, Canada

[6]Alfred Wegener Institute for Polar and Marine Research, Am Handelshafen 12, Bremerhaven 27568, Germany

[7]Earth System Science Interdisciplinary Center, University of Maryland Research Park (M-Square), 5825 University Research Ct, Ste 4001, College Park, Maryland 20740, USA

[8]*Present address:* Department of Biological Sciences, University of Southern California, 3616 Trousdale Parkway, Los Angeles, California 90089, USA

[9]*Present address:* Aix-Marseille Université, CNRS, LOB-UMR 6535, Laboratoire d'Océanographie et de Biogéochimie, OSU/Centre d'Océanologie de Marseille, 163 Avenue de Luminy, 13288 Marseille Cedex 09, France

[10]*Present address:* CNRS (CNRS/INSU), UMR 6535, Campus de Luminy Case 901, 163 Avenue de Luminy, 13288 Marseille Cedex 09, France

[11]*Present address:* Biology Department, MS #32, Woods Hole Oceanographic Institution, 266 Woods Hole Road, Woods Hole, Massachusetts 02543, USA

[12]*Present address:* Department of Biological Sciences, The University of Nebraska, 204 Morrison Center Lincoln, Nebraska 68583-0900, USA

[13]*Present address:* Department of Chemistry, Trent University, 1600 West Bank Drive, Peterborough, Ontario K9J 7B8, Canada

ABSTRACT: The North Atlantic spring bloom is one of the largest annual biological events in the ocean, and is characterized by dominance transitions from siliceous (diatoms) to calcareous (coccolithophores) algal groups. To study the effects of future global change on these phytoplankton and the biogeochemical cycles they mediate, a shipboard continuous culture experiment (Ecostat) was conducted in June 2005 during this transition period. Four treatments were examined: (1) 12°C and 390 ppm CO$_2$ (ambient control), (2) 12°C and 690 ppm CO$_2$ (high pCO$_2$), (3) 16°C and 390 ppm CO$_2$ (high temperature), and (4) 16°C and 690 ppm CO$_2$ ('greenhouse'). Nutrient availability in all treatments was designed to reproduce the low silicate conditions typical of this late stage of the bloom. Both elevated pCO$_2$ and temperature resulted in changes in phytoplankton community structure. Increased temperature promoted whole community photosynthesis and particulate organic carbon (POC) production rates per unit chlorophyll *a*. Despite much higher coccolithophore abundance in the greenhouse treatment, particulate inorganic carbon production (calcification) was significantly decreased by the combination of increased pCO$_2$ and temperature. Our experiments suggest that future trends during the bloom could include greatly reduced export of calcium carbonate relative to POC, thus providing a potential negative feedback to atmospheric CO$_2$ concentration. Other trends with potential climate feedback effects include decreased community biogenic silica to POC ratios at higher temperature. These shipboard experiments suggest the need to examine whether future pCO$_2$ and temperature increases on longer decadal timescales will similarly alter the biological and biogeochemical dynamics of the North Atlantic spring bloom.

KEY WORDS: Ocean acidification · Global change · Carbon dioxide · Temperature · Coccolithophores · Diatoms · Calcification · North Atlantic bloom

*Corresponding author. Email: dahutch@usc.edu

INTRODUCTION

Of the many ongoing global anthropogenic-change processes, increased atmospheric CO_2 and rising temperatures are likely to have some of the most profound effects on ocean biology and biogeochemistry. Atmospheric CO_2 concentration is currently increasing by about 0.4 % yr^{-1}, and has already increased by about 30 % over pre-industrial levels. It has been predicted that atmospheric partial pressure of CO_2 (pCO_2) will be >700 ppm by the end of this century (Alley et al. 2007). This will lead to a projected seawater CO_2 concentration increase of about 30 μmol kg^{-1} and a corresponding seawater pH decrease to about 7.8, roughly 0.3 units lower than today's value (Wolf-Gladrow et al. 1999). At the same time, warming associated with the release of greenhouse gases into the atmosphere has been predicted to raise sea surface temperature (SST) by 1 to 4°C over the next 100 yr (Bopp et al. 2001, Alley et al. 2007).

These global changes will have major effects on the physiology of marine phytoplankton (Boyd & Doney 2002, Hays et al. 2005). For instance, it has been shown that CO_2 enrichment will significantly influence the photosynthesis, elemental composition, and calcification of marine phytoplankton (Riebesell 2004). Furthermore, these effects are taxon specific, so future phytoplankton community structure and succession should also be influenced (Tortell et al. 2002, Hare et al. 2007). Phytoplankton metabolic activity could be accelerated by elevated temperature (Eppley 1972); therefore, rising SST will also have important effects on marine phytoplankton. Laboratory studies have predicted that CO_2 enrichment, together with rising temperature, may have interactive influences on some phytoplankton species (Fu et al. 2007, Hutchins et al. 2007, Feng et al. 2008). However, there is little information available on the effects of simultaneously increased temperature and pCO_2 on natural phytoplankton communities (Hare et al. 2007).

The intense annual North Atlantic spring bloom is one of the most dramatic and predictable biological events in the world's oceans (Esaias et al. 1986). Typically, this bloom follows a succession in which initial dominance by diatoms later gives way to nanoplankton, mainly coccolithophores (Lochte et al. 1993). This secondary coccolithophore bloom may be induced by high light conditions (Tyrrell & Taylor 1996), silicate depletion during the early diatom-dominated bloom phase (Sieracki et al. 1993), phosphate becoming more limiting than nitrate (Riegman et al. 1992, Tyrrell & Taylor 1996), low dissolved CO_2, and high carbonate saturation state (Tyrrell & Merico 2004), or some combination of these factors. How community structure, phytoplankton succession, and marine biogeochemical cycles during this annual event will change as a result of increasing future CO_2 concentration and SST is still unknown. The North Atlantic is thus an ideal regime in which to examine experimentally how global changes could drive future shifts in phytoplankton diversity and in the resulting patterns in carbon and nutrient biogeochemistry.

The goals of the present study were to investigate the individual and combined effects of increased pCO_2 and temperature on algal community structure, phytoplankton succession, and elemental cycling in the North Atlantic spring bloom area. To do this, we conducted a shipboard continuous culture incubation ('Ecostat'; Hare et al. 2005, 2007) using a natural North Atlantic bloom phytoplankton community. Unlike short-term bottle growout experiments (days), this shipboard adaptation of methods of laboratory continuous culture systems offers the possibility of effectively simulating natural environmental changes under controlled experimental conditions using a natural phytoplankton community growing at near steady state in longer incubations (weeks; Hutchins et al. 2003, Hare et al. 2005, 2007). The results of this large collaborative experiment are presented in 3 companion papers. This paper mainly discusses the phytoplankton community and biogeochemical responses. The companion paper Rose et al. (2009, this volume) focuses on microzooplankton dynamics, and Lee et al. (2009, this volume) largely deals with dimethylsulfoniopropionate (DMSP) production.

MATERIALS AND METHODS

Experimental setup and sampling. The shipboard incubation was conducted between 20 June and 14 July 2005 on the RV 'Seward Johnson II' during the NASB 2005 cruise. The initial phytoplankton community was collected at 57.58°N, 15.32°W (temperature: 12.0°C, salinity: 35.3). A shipboard continuous culture incubation system ('Ecostat') was used to carry out steady-state simulation experiments under defined projected pCO_2 and temperature conditions (Hutchins et al. 2003, Hare et al. 2005, 2007). Near-surface water (5 to 10 m) containing the intact North Atlantic bloom community was collected into a 50 l mixing carboy using a trace-metal-clean, towed-intake surface water Teflon diaphragm pumping system (Bruland et al. 2005) and then was cleanly filtered through acid-washed 200 μm Nitex mesh to eliminate large zooplankton. The whole water was then dispensed into 24 acid-washed clean, 2.7 l, clear polycarbonate bottles for incubation. Clean 50 l seawater medium reservoirs were filled with 0.2 μm in-line filtered seawater collected at the same time as the whole phytoplankton

community, which was later used as medium for dilution during the continuous culture incubation.

Initial nutrient concentrations in the collected water were low, at 0.32 µM nitrate, 0.12 µM phosphate, and 0.7 µM silicate. Modest levels of nitrate and phosphate (final concentrations 5 and 0.31 µM, respectively) were therefore added to the medium and initial incubation bottles, yielding final dissolved molar ratios of 0.13 for Si:N and 0.08 for Si:P. The phytoplankton community that we sampled was well into the transition phase from diatoms to coccolithophores, so silicate limitation in the incubation system accurately reproduced typical nutrient conditions at this time (Sieracki et al. 1993). At most stations along our cruise track, near-surface nitrate concentrations were 2 to 5 µM and phosphate concentrations were 0.2 to 0.5 µM, but silicate levels were only 0.2 to 0.7 µM (Leblanc et al. 2009). Thus, nearly the entire region at the time of our study was characterized by low dissolved Si:N ratios of 0.1 to 0.2. Because the station where we collected water for our experiments was somewhat atypical (N and P depleted to an unusual extent), our nutrient additions were intended to simply reproduce the more usual values we saw during the cruise. Although it should be noted that adding N and P without Si would tend to select against diatoms, our intention was not to provide a level playing field for all algal taxa. Rather, we tried to simulate accurately the normal biogeochemical and biological conditions in the late part of the North Atlantic spring bloom.

Two Ecostat systems were used to examine 4 treatments—(1) ambient: 12°C and 390 ppm CO_2; (2) high CO_2: 12°C and 690 ppm CO_2, with only pCO_2 increased; (3) high temperature: 16°C and 390 ppm CO_2, with only temperature increased; and (4) greenhouse: 16°C and 690 ppm CO_2, with both temperature and pCO_2 increased simultaneously. To provide for robust statistical testing of treatment effects, 6 replicate bottles were used for each of the 4 treatments. The 2 incubation temperatures were controlled using a recirculating thermoregulation system consisting of a thermostat-controlled heat-exchange cooling system and in-line electric heaters. One of the Ecostats was maintained using this system at ambient SST (12°C) and the other was 4°C above ambient temperature, as has been predicted for high latitude ocean regimes by the year 2100 (Sarmiento et al. 1998, 2004). Two pCO_2 levels were set by gentle bubbling (3 ml min^{-1}) of ambient air (~390 ppm CO_2) and a HEPA-filtered commercially prepared air/CO_2 mixture (690 ppm CO_2). Ambient air was collected using an air pump with a HEPA-filtered intake near the ship's bow, to avoid the ship's exhaust gases. CO_2 equilibration was monitored throughout the experiment using both pH and dissolved inorganic carbon (DIC) measurements. The

light levels of the incubators were adjusted using a combination of spectrally corrected blue plastic (Hutchins et al. 1998) and neutral-density shade screens, to provide an irradiance of 30% of the incident sea surface level (I_0) inside the incubators.

The incubation was conducted in 'batch' growth mode for the first 3 d (T0, T1, and T2) without dilution of filtered seawater medium. The continuous incubation started on the fourth day (T3), with a constant dilution rate of 0.5 d^{-1}, which is within the typical range for whole phytoplankton community growth rates in this area (Gaul et al. 1999). The incubation lasted until the final sampling day on T14. The dilution rate of each bottle was adjusted individually by a separate peristaltic pump, with an inflow line going into the bottle from the top of the cap. The outflow tubing was connected at the shoulders of the bottles and drained down through a port in the incubator side along outflow lines and finally into the enclosed outflow receiving bottles, which were kept dark in a closed container. All parts of the system were built of either Teflon or polycarbonate and were rigorously acid cleaned prior to the experiment. The system was equipped with a compressed air-driven system to gently rotate the entire Plexiglas rack holding the Ecostat bottles inside the incubator through a 120° arc on a timed cycle (5 to 15 min) to ensure that the phytoplankton cells remained suspended in the bottles (Hutchins et al. 2003, Hare et al. 2005, 2007).

Daily sampling directly from the Ecostat bottles was limited to ~10% of the bottle volume, to avoid significant perturbations of the nutrient input/biomass accumulation equilibrium. Due to this sampling volume limitation, daily samples were only taken for the measurements requiring relatively small volumes. These included chlorophyll a (chl a) and dissolved nutrients (nitrate, phosphate, and silicate) daily, except for T7 and T13; algal community structure (flow cytometry and microscopic cell counts) on T0, T2, T6, T11, and T14; DIC on T0, T4, T8, T10, and T14; bacteria and virus counts on T0, T2, T5, T8, T11, and T14; and pCO_2 on T0, T7, and T13, for which samples were taken directly from the bottles with a sampling syringe. Algal composition by high-performance liquid chromatography (HPLC), particulate organic carbon (POC), biogenic silica (BSi) and particulate organic nitrogen (PON) samples were taken on T0 and T14. On the final day (T14), all the samples were taken directly from the incubation bottles.

Seawater carbonate system measurements. Samples for DIC measurements were taken in 20 ml borosilicate vials (Fisher Scientific) and were fixed with 0.2 ml of a 5% $HgCl_2$ solution. The vials were sealed and stored at 4°C until analysis. DIC was measured in an acid-sparging instrument (Walz & Friederich 1996). For analyses,

1.25 ml samples were injected into a sparging column, where the CO_2 resulting from acid conversion of the DIC pool was quantified using a LiCor infrared analyzer with high precision flow control; replicate precision for seawater samples is about ±0.06%. pCO_2 was measured using a membrane inlet mass spectrometer (MIMS; Hiden Analytical), following the methods presented in Gueguen & Tortell (2008).

Phytoplankton community and biomass analyses. Size-fractionated chl *a* samples were filtered at low vacuum onto 0.2 and 2 μm polycarbonate filters (Millipore), extracted in 90% acetone at –20°C in the dark for 18 to 24 h, and measured with a Turner 10-AU fluorometer (Welschmeyer 1994). Samples (400 to 1000 ml) for taxon-specific pigments were filtered onto GF/F filters (Whatman) under low vacuum at sea and were immediately frozen in liquid nitrogen for later HPLC analysis in the laboratory. Photosynthetic pigments were separated on an automated Hewlett Packard 1050 HPLC system using a reverse-phase Waters Symmetry C-8 column and a solvent gradient containing methanol, aqueous pyridine, acetone, and acetonitrile (Zapata et al. 2000, DiTullio & Geesey 2002). A diode array detector recorded pigment spectra every 5 s over the wavelengths 350 to 600 nm and continuous chromatograms at 410, 440, and 455 nm. A HP 1046A fluorescence detector with excitation of 421 nm and emission at 666 nm (optimized for chl *a*) was also used to identify and quantify chl *a* and *c*. The system was calibrated by repeated injections of pigment standards isolated from a variety of unialgal cultures maintained in the laboratory (DiTullio & Geesey 2002).

Phytoplankton cell abundance was determined on preserved samples by both microscopy and flow cytometry. Samples of 50 or 100 ml for laboratory cell counts using microscopy were preserved by a final concentration of 1% glutaraldehyde and stored at 4°C in the dark until analysis. Phytoplankton taxonomy and cell abundance of larger microphytoplankton species were determined microscopically with a 2 mm Spears-Levy counting chamber. Before microscopic analysis, the samples were concentrated as described in Hare et al. (2005, 2007).

Virus and bacterial abundance. Virus and bacterial abundance were determined by first preserving the unfiltered water in 2% final glutaraldehyde and then preparing the slides at sea (Wen et al. 2004). For virus enumeration, 850 μl of sample collected on 0.02 μm nominal pore size 25 mm Anodisc filters (Whatman) was stained with SYBR Green (Noble & Fuhrman 1998). For bacteria enumeration, cells stained with Acridine Orange were collected on 0.2 μm nominal pore size 25 mm black polycarbonate filters (Osmonics) (Hobbie et al. 1977). All slides were stored at –20°C until virus-like particles could be enumerated by epi-

flourescence microscopy (Leica DMRXA with a 'wide blue' filter set [λ_{Ex} = 450 to 490 nm and λ_{Em} = 510 nm]).

Dissolved and particulate matter. Dissolved nutrient samples were taken by syringe directly from the incubation bottles. Samples were immediately 0.2 μm filtered and stored at –20°C. Samples were analyzed in the laboratory using a Flo-Solution IV analyzer (O/I Analytical). Total particulate carbon (TPC) was measured by filtering 100 to 200 ml samples onto pre-combusted (450°C, 2 h) 25 mm diameter Whatman GF/F glass fiber filters, which were then dried at 55°C. For POC analysis, the TPC filters were fumed for 3 h to remove all the inorganic carbon. PON and POC were then measured by an Elemental 270 Combustion System (Costech Analytical Technologies).

BSi samples (100 to 200 ml) were filtered onto 0.6 μm, 47 mm polycarbonate filters, dried at 60°C at sea, and then stored at room temperature until analysis. The samples were analyzed in the laboratory following the method of Brzezinski & Nelson (1995). The concentration of transparent exopolymer particles (TEP) was determined as described in Passow & Alldredge (1995).

Photosynthesis–irradiance curves. Photosynthesis–irradiance response (*P-E*) curves were obtained by measuring primary productivity as a function of light intensity by the ^{14}C uptake method on a radial photosynthetron similar to the design described by Babin et al. (1994). Approximately 750 ml of sample was inoculated with 2 mCi of $Na_2^{14}CO_3$ (Nordion) in a 2 l acid-cleaned polycarbonate flask. Following gentle homogenization, 50 ml aliquots were then automatically dispensed into 36 acid-cleaned 60 ml polycarbonate culture flasks. The flasks were then incubated in triplicate on the photosynthetron at 12 different irradiances at the appropriate temperature (12 or 16°C) for 2 h. The irradiance source was an Osram metal halide bulb. Irradiance was measured before and after incubation using a Biospherical Instruments QSL-100 quantum meter. Time zero ^{14}C uptake rates were measured and subtracted from all experimental samples. After homogeneously mixing the 2 l flask, triplicate samples (100 μl) for total ^{14}C activity (T_A) were taken and added to a 7 ml scintillation vial containing 100 μl of a phenethylamine:MeOH (1:1) solution. Then, 4 ml of scintillation fluid (Ecolume) was added to the vials before determining the total radioactivity. After the 2 h incubation, samples were immediately filtered and degassed overnight with 10% HCl, and then counted on a Beckman 6500 LSC corrected for quench using the external standards ratio. Photosynthetic rates were calculated from T_A, final radioactivity, and total DIC concentrations. The curves were fitted using the 3-parameter model of Platt & Gallegos (1980).

POC and PIC production. POC and PIC production rates were estimated with the micro-diffusion tech-

nique according to Paasche & Brubak (1994), with some modifications. Briefly, PIC was separated from the organic carbon by dissolving the calcite in H_3PO_4 and trapping the liberated $^{14}CO_2$ in a filter wetted with viscous organic base in a closed scintillation vial. The 2 fractions were radio-assayed separately. Samples (75 ml) were incubated with 10 μCi $NaH^{14}CO_3$ added for 24 h under the appropriate experimental conditions for each treatment inside the Ecostat incubators. Incubations were started after the daily sampling at noon (1300 h). After incubation, the samples were filtered onto 25 mm diameter Whatman GF/F glass fiber filters. The filters were placed into 20 ml scintillation vials with a plastic rim on the inside of the caps, and then 13 mm Gelman AE GF glass fiber filters (Pall Corporation) were wetted with 200 μl of phenethylamine and attached on the caps. One milliliter of 50% phosphoric acid was added to each vial, which was immediately air-tightened with the cap containing the basic filter. After incubation overnight on a shaker table, the 2 fractions were radio-assayed separately.

Statistics. Significance tests were conducted with ANOVA F, as described in Rose et al. (2009). Before carrying out the tests, outliers were removed using the Hampel identifier, as modified by Rousseeuw & van Zomeren (1990). Results for all analyses are presented as the mean and standard deviation of 6 replicate samples for each treatment.

RESULTS

The gentle bubbling protocol maintained the seawater carbonate buffer system in a relatively stable condition in the incubation bottles in each treatment during the course of the experiment. Total DIC was ~2100 and ~2250 μmol kg^{-1} in the low pCO_2 and high pCO_2 treatments, respectively, in the 12°C temperature treatment bottles. DIC ranged from 2000 (low pCO_2) to 2180 μmol kg^{-1} (high pCO_2) in the 16°C bottles. The original pCO_2 of the collected seawater was 395 ± 3 ppm, as measured by MIMS. After the bubbling started, pCO_2 values measured in the 2 low pCO_2 treatments were 390 ± 8 ppm on T7 and T13. In the 2 high pCO_2 treatments, however, the levels were 688 ± 2 ppm, somewhat lower than the projected 750 ppm, likely due to biological CO_2 uptake in those treatments.

Phytoplankton biomass estimated as chl a responded to elevated temperature and pCO_2 (Fig. 1A). Total chl a concentration increased in all treatments and doubled in the greenhouse treatment over the first 3 d of the experiment, during the batch incubation mode. As dilution began after T3, chl a concentrations started to decline and returned to near-initial levels by T8.
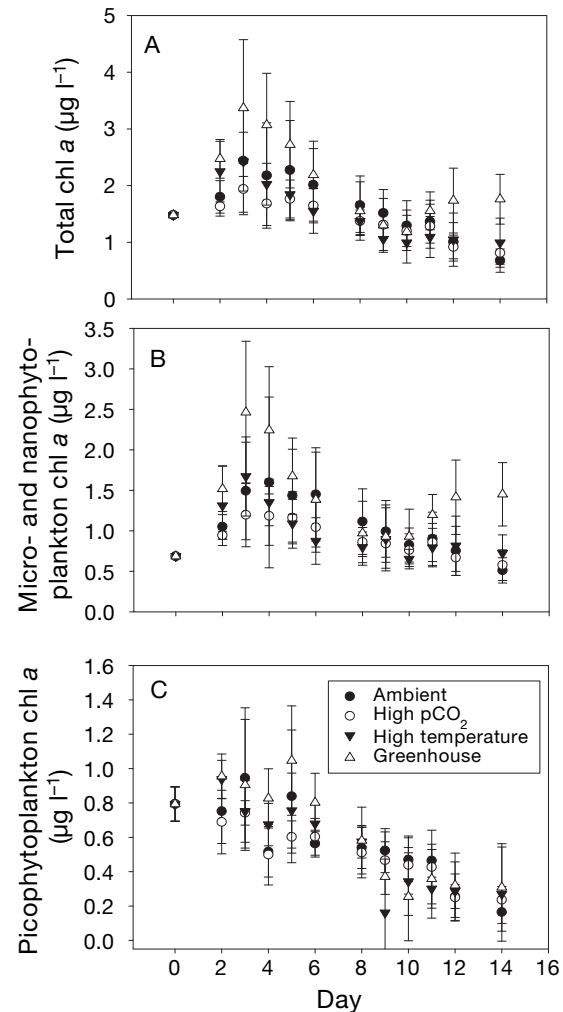

Fig. 1. Chl a concentrations of (A) the total community, (B) microphytoplankton and nanophytoplankton (>2.0 μm), and (C) picophytoplankton (0.2 to 2 μm) in the 4 incubation treat-ments (see 'Materials and methods: Experimental setup and sampling' for details). Error bars represent SD (n = 6)

Thereafter, chl a levels were relatively stable until the final day (T14), with an average concentration close to the initial value, indicating that the net growth rate (i.e. including grazing) of the total phytoplankton community was in balance with the dilution rate. During the final 3 d, chl a biomass was highest in the greenhouse treatment relative to the other treatments ($p < 0.05$; Fig. 1A).

During the incubation period, size-fractionated chl a concentrations (Fig. 1B,C) and cell densities estimated by flow cytometry (Rose et al. 2009) suggested that nano- and microphytoplankton came to comprise the majority of the whole phytoplankton community biomass in all of the treatments. Size-fractionated chl a biomass associated with picophytoplankton declined
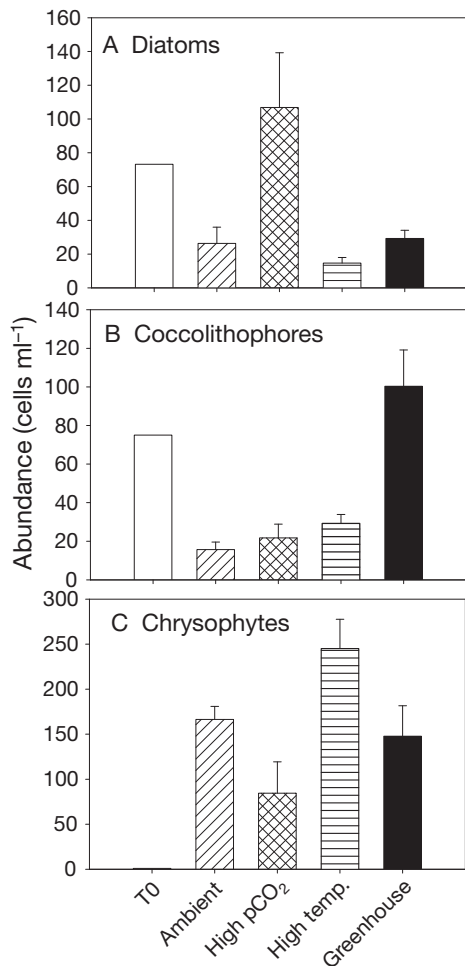
Fig. 2. Microphytoplankton abundance on the initial day (T0) and in the 4 treatments on the final day (T14). (A) diatoms, (B) coccolithophores, and (C) chrysophytes. Error bars represent SD (n = 6)

Fig. 3. Ratios of *Pseudo-nitzschia* sp. and *Cylindrotheca* sp. cell abundances on the initial day (T0) and in the 4 treatments on the final day (T14). Error bars represent SD (n = 6)

during the course of the experiment to <0.2 µg l^{-1}, and there were no significant differences (p > 0.05) among treatments (Fig. 1C). The changes in micro- plus nanophytoplankton chl *a* (Fig. 1B) were similar to changes in total chl *a* (Fig. 1A). This large-size-fraction chl *a* showed an initial increase during batch mode (especially in the greenhouse treatments), followed by a decline to near-initial values in all treatments, with the highest final levels in the greenhouse bottles (p < 0.05). Detailed descriptions of changes in chl *a* biomass, algal community composition measured with flow-cytometry, and the microzooplankton community are presented in Rose et al. (2009).

Microscopy cell counts of microphytoplankton on the final day (T14) further demonstrated different effects of increased temperature and pCO$_2$ on different phytoplankton groups (Fig. 2). The 3 main phytoplankton groups observed during the incubation were diatoms, coccolithophores, and chrysophytes. On the initial
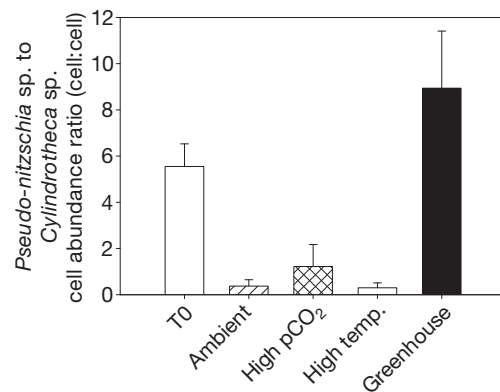
day (T0), haptophytes (mainly coccolithophores) were dominant in the phytoplankton community based on the phytoplankton pigment analyses (53% of the total algal chl *a*; Lee et al. 2009). In the microphytoplankton group, total diatom abundance on the final sampling day (T14) increased dramatically in the high pCO$_2$ treatment relative to that in the 3 other treatments (>3-fold; Fig. 2A). All 4 treatments were dominated by the same 2 pennate diatom species on the final sampling day, *Pseudo-nitzschia* sp. and *Cylindrotheca* sp. (Fig. 3). The ratios of *Pseudo-nitzschia* sp. to *Cylindrotheca* sp. cell abundance were 0.37 ± 0.28 (ambient), 1.22 ± 0.95 (high pCO$_2$), 0.30 ± 0.21 (high temperature), and 8.94 ± 2.47 (greenhouse) (Fig. 3). These values suggest that the relative abundance of the slightly larger *Pseudo-nitzschia* sp. was much higher at higher pCO$_2$. Thus, the larger species was more dominant after CO$_2$ enrichment, especially when combined with increased temperature in the greenhouse treatment.

On the final day, coccolithophore abundance in the greenhouse treatment was significantly higher than that in the 3 other treatments and 5-fold higher than that in the ambient treatment (p < 0.05, ANOVA; Fig. 2B), which was also supported by the flow-cytometry results (identified based on side scatter, forward scatter, and chlorophyll fluorescence; data not shown). The cell abundance of chrysophytes was very low on T0 and increased in all 4 of the treatments during the time course of the incubation. Chrysophyte cell density on the final day was significantly higher (p < 0.05) at elevated temperature and lower (p < 0.05, ANOVA) at elevated pCO$_2$ in each temperature treatment (Fig. 2C). This effect of pCO$_2$ was not observed for diatoms or coccolithophores (Fig. 2A,B).

On the final day, averaged 19-hexanoyloxyfucoxanthin (19-hex) concentration (indicative of haptophytes, in this case coccolithophores) was highest in the greenhouse treatment (Fig. 4; Lee et al. 2009). The final day
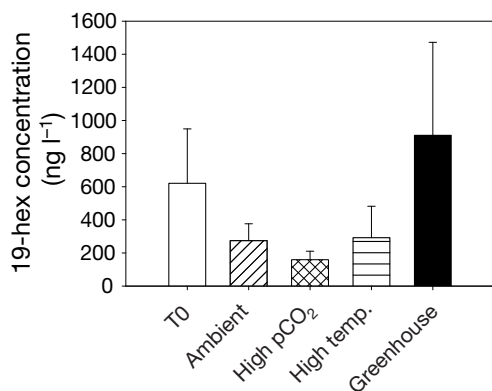
Fig. 4. Concentration of the haptophyte pigment 19-hexanoyl-oxyfucoxanthin (19-hex, primarily from coccolithophores) on the initial day (T0) and in the 4 treatments on the final day (T14). Error bars represent SD (n = 6)
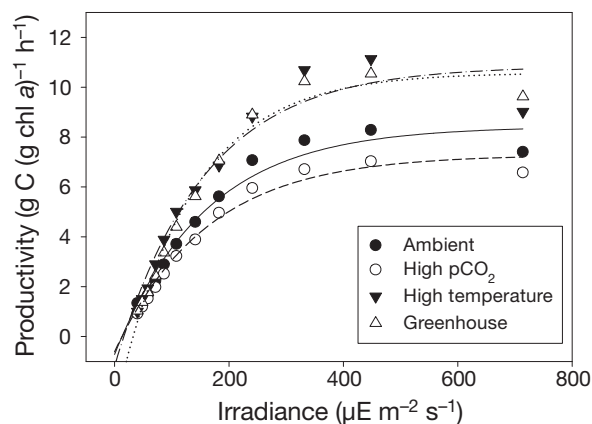

Fig. 5. Photosynthesis versus irradiance curves for the 4 treatments on the final day (T14) (triplicates combined). Note: curves representing high temperature and greenhouse treatments are dotted and dash-dotted, respectively

19-hex concentration was about 3-fold higher in the greenhouse than in the ambient treatment. However, due to both sampling and experimental variability, this increase was not statistically significant. The results from bacterial and viral counts suggested low abundances of bacteria and viruses during the course of the experiment, with no apparent treatment-related trends (data not shown).

Photosynthetic carbon fixation also responded to the experimental treatments (Fig. 5). *P-E* curves on the last day of the incubation demonstrated that maximum chl *a*-normalized photosynthetic rates (P_{max}^B) increased significantly from an average value of 8.2 to 12.8 g C (g chl *a*)$^{-1}$ h^{-1} in the 2 higher temperature treatments compared to the other 2 ambient temperature treatments (Fig. 5). Increased pCO$_2$ alone decreased P_{max}^B slightly only at ambient temperature. The initial slope of the *P-E* curves (α, with values of 0.057, 0.049, 0.077, and 0.103 g C h^{-1}(g chl *a*)$^{-1}$(µE m^{-2} s^{-1})$^{-1}$ for ambient, high pCO$_2$, high temperature, and greenhouse treatments, respectively) was also increased significantly in the high temperature and greenhouse treatments (p < 0.05) with respect to ambient conditions.

Dissolved nutrients in the incubation bottles reached stable levels without strong treatment-related trends (data not shown). By the middle of the experiment, nitrate had stabilized at 2 to 3 µM, phosphate at 0.1 to 0.2 µM, and silicate at 0.2 to 0.5 µM in all treatments; these steady-state concentrations are quite similar to those we measured in the water column at numerous stations during the cruise (Leblanc et al. 2009). As intended in the experimental design, silicate was depleted the most, although none of the nutrients were ever fully depleted in any treatment.

The BSi:POC molar ratio on the final day in all 4 treatments decreased compared to the T0 value. On the final day, the ratio was significantly lower (p < 0.05)
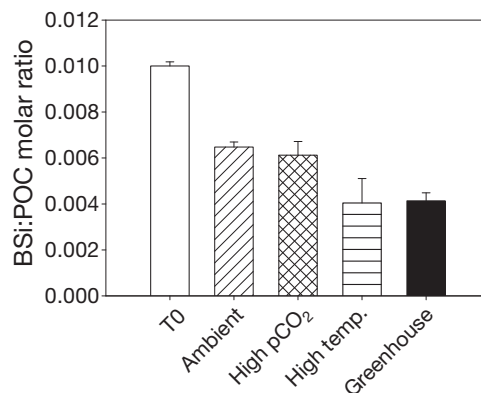

Fig. 6. Cellular biogenic silica (BSi) to particulate organic carbon (POC) ratios on the initial day (T0) and in the 4 treatments on the final day (T14). Error bars represent SD (n = 6)

in the high temperature and greenhouse treatments than it was in the 2 lower temperature treatments (Fig. 6). The molar ratio dropped by 30% (from ~0.006 to 0.004) after the temperature was increased by 4°C. However, within the same temperature conditions, there was no significant difference (p > 0.05) between either the ambient and high pCO$_2$ treatments or the high temperature and greenhouse treatments (Fig. 6). A similar trend was observed with BSi:PON molar ratios, and POC, PON, and BSi concentrations in all treatments were relatively stable for the second half of the experiment (data not shown).

On the final day, chl *a*-normalized production rates of POC and PIC varied as a function of temperature and pCO$_2$ (Fig. 7), and both were increased compared to T0. The POC production rate was significantly higher in the 2 high temperature treatments—high temperature and greenhouse—(p < 0.05;
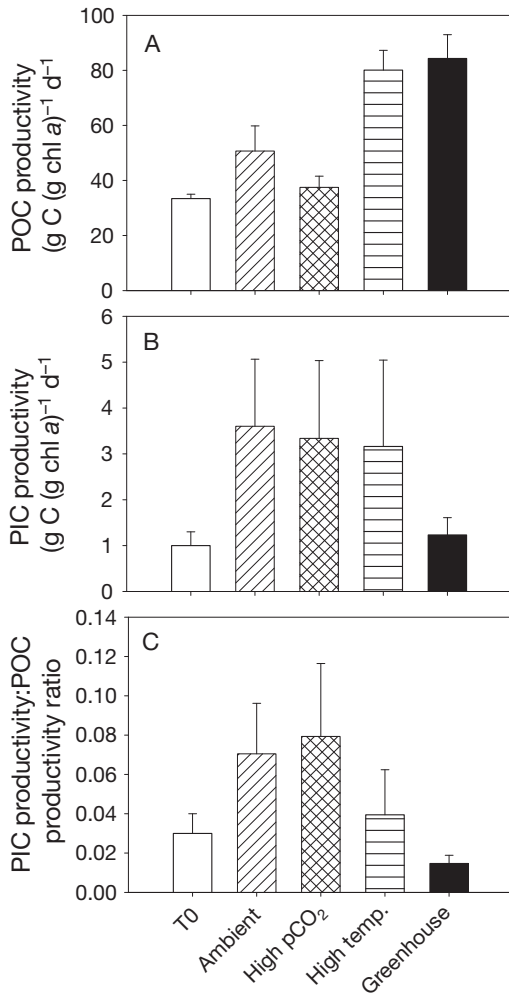
Fig. 7. Production of (A) particulate organic carbon (POC) and (B) particulate inorganic carbon (PIC) on the initial day (T0) and in the 4 treatments on the final day (T14), and (C) the PIC:POC productivity ratio on the initial day and in the 4 treatments on the final day. Error bars represent SD (n = 6)

Fig. 7A). The highest value of POC production was observed in the greenhouse treatment. However, despite the cell abundance of coccolithophores being highest in the greenhouse treatment (Fig. 2A), the PIC production rate was greatly reduced in these samples (Fig. 7B; $p < 0.05$). Increased pCO_2 alone (the high pCO_2 treatment) did not influence PIC productivity compared with the ambient treatment. Due to the decreased PIC productivity and increased POC productivity in the greenhouse treatment, the ratio of PIC:POC productivity on the final sampling day was lowest in the greenhouse treatment (Fig. 7C; $p < 0.05$). There was no significant difference between the other treatments (Fig. 7C; $p > 0.05$). For C:N:P ratios, TEP concentrations, and TEP:POC ratios, there were no significant differences among the 4 treatments (data not shown).

DISCUSSION

The North Atlantic spring bloom phytoplankton community responded significantly to the experimental treatments in this shipboard continuous incubation experiment. Treatment-specific community shifts were induced by both increased temperature and pCO_2 conditions, with the highest diatom abundance in the high CO_2 treatment, the highest coccolithophore abundance in the greenhouse treatment, and the highest chrysophyte abundance at high temperature. Both photosynthetic parameters and POC productivity normalized to chl *a* were greatly promoted by elevated temperature. In contrast, net calcification (PIC production) decreased significantly in the greenhouse treatment. Consequently, the potential marine rain ratio (as estimated by the ratio of PIC:POC production) was significantly lower when temperature and pCO_2 were elevated simultaneously, suggesting the possibility of a reduced export ratio of calcium carbonate relative to organic carbon in the future marine environment.

These CO_2 and temperature effects during our experiment were superimposed on a phytoplankton community that was first structured by nutrient availability in all treatments. We intentionally set up our experiment to be Si-limited, thus closely reproducing the biogeochemical conditions that prevailed throughout the region during our cruise (Leblanc et al. 2009). This experimental design undoubtedly favored coccolithophores over diatoms, especially since half-saturation constants for diatom growth on silicate can be relatively high (Martin-Jezequel et al. 2000). Because the concentrations and ratios of nutrients supplied to all 4 treatments were identical though, differential nutrient supply cannot be the reason for the observed CO_2/temperature treatment effects. These nutrient concentrations and ratios were typical of those we observed throughout the area at the time of our study (Leblanc et al. 2009); thus, nutrient influences on community structure in our experiments should have been similar to those operating on the *in situ* community of the late North Atlantic bloom.

During the last few days of this incubation experiment, parameters such as chl *a* biomass, POC, and BSi were nearly constant in most treatments, indicating that community net growth was roughly balanced by the losses through the outflow. Although these bulk parameters reached something approximating steady state, community composition may or may not have reached a real equilibrium during the course of our 2 wk experiment, as this can often take longer to stabilize than bulk chl *a* (Tilman 1977). Nevertheless, the major advantage of the Ecostat system over traditional 'growout' experiments is that the steady low-level supply of nutrients allows much longer time periods for the

community to acclimate to the experimental conditions (Hare et al. 2005, 2007). This shipboard 'greenhouse ocean' simulation was still necessarily a relatively short-term study compared to expected decadal-scale changes in global pCO$_2$ and temperature. Therefore, this experiment cannot replicate any possible long-term adaptation and evolution of marine phytoplankton groups (Hutchins et al. 2003, Hare et al. 2007). As in all bottle incubations, grazing by large zooplankton and particle sinking were excluded, which are also important environmental factors. Changes in these top-down control and export loss factors will likely also play salient roles in structuring future phytoplankton communities.

Despite these qualifications, this type of shipboard incubation experiment is uniquely suited to provide us with a detailed perspective on how the current dominant phytoplankton groups in the North Atlantic spring bloom may respond to bottom-up control by projected future pCO$_2$ and temperature changes. Although too short to incorporate long-term biological adaptation processes, these experiments nevertheless offer valuable insights into which groups within the current phytoplankton community are already poised to benefit (or suffer) under expected future ocean conditions. In this way, manipulative experiments offer an additional tool to complement, enhance, and extend the knowledge of ocean global change effects that is obtained from laboratory studies, time series stations, long-term observations, and quantitative modeling efforts (Hare et al. 2007).

Our experimental results indicated that a 4°C temperature elevation induced higher chl *a*-normalized carbon fixation rates by the North Atlantic phytoplankton community. POC production normalized to chl *a* on the final sampling day was 2-fold higher at the higher temperature than in the lower temperature treatments. Maximum photosynthetic rates normalized to chl *a* and the slope of the light-limited portion of the *P-E* curve also displayed similar trends. At the same time, the final chl *a* biomass was highest in the greenhouse treatment. The dark reactions of photosynthesis are enzymatically mediated and are thus known to be especially sensitive to temperature (Geider & Osborne 1992).

Previous studies have shown similar results, in that modestly increased temperature greatly promoted phytoplankton photosynthetic parameters in laboratory cultures of marine cyanobacteria (Hutchins et al. 2007, Fu et al. 2007) and the coccolithophorid *Emiliania huxleyi* (Feng et al. 2008). Growth rates of phytoplankton in general have long been known to scale closely with temperature (Eppley 1972, Banse 1991). Recent shipboard continuous incubation experiments similar to ours that used Bering Sea natural phyto-

plankton communities also found that chl *a*-normalized maximum carbon fixation rates could potentially double with expected surface ocean warming trends over the next 100 yr (Hare et al. 2007). This suggests possible accelerated carbon sequestration by marine phytoplankton from the atmospheric CO$_2$ reservoir. Such trends could offer a potential negative feedback on atmospheric CO$_2$ and greenhouse warming, although this also depends on the ability of the community to export this additional fixed carbon. This also assumes that photosynthesis is not limited by other factors such as nutrients or light, which may also change along with temperature if surface ocean stratification intensifies in the future. In contrast to higher temperature, increased pCO$_2$ alone had relatively little effect on community carbon fixation in our study, which is similar to the results from previous experimental studies in the tropical North Pacific (Tortell et al. 2002) and the Bering Sea (Hare et al. 2007).

These increased carbon fixation rates were also accompanied by large phytoplankton community structure changes. By far the most striking shift was a greatly increased abundance of coccolithophores in the combined high temperature and pCO$_2$ environment (greenhouse treatment). The current seawater CO$_2$ concentration is below the saturation level for photosynthesis by marine coccolithophores (Riebesell et al. 2000, Rost et al. 2003). Our results reflected trends that were similar to those seen in these aforementioned studies, indicating that coccolithophores will benefit from rising atmospheric pCO$_2$.

The trend towards coccolithophorid dominance was dramatically enhanced when temperature and pCO$_2$ were increased simultaneously in the greenhouse treatment. The coupled influence of increased temperature and pCO$_2$ on coccolithophorid growth and physiology was also found in laboratory culture experiments with *Emiliania huxleyi*, in which photosynthetic carbon fixation was greatly promoted when both temperature and pCO$_2$ were increased together (Feng et al. 2008). However, the physiological mechanisms driving these results are still unknown.

In contrast, some previous work has suggested that the photosynthetic carbon fixation rate of marine diatoms is close to saturation at the present day CO$_2$ level (Burkhardt et al. 1999, 2001, Rost et al. 2003). However, overall diatom abundance also increased after CO$_2$ enrichment in our experiments, especially in the high pCO$_2$ treatment at ambient temperature. Despite this trend with increased CO$_2$ alone, large dominance shifts within the diatom community did not occur in this treatment, but in the greenhouse treatment instead, where the combination of higher temperature and pCO$_2$ together strongly favored the genus *Pseudo-nitzschia* over *Cylindrotheca*. CO$_2$-

mediated shifts from smaller pennate to larger centric diatoms have been documented in manipulative experiments in the Ross Sea, Antarctica, where they have been suggested to potentially affect carbon export (Tortell et al. 2008, Feng et al. unpubl. data). The species composition shifts between the 2 pennates in our greenhouse treatment could be less likely to lead to significant carbon export differences since *Pseudo-nitzschia* sp. is only slightly larger than *Cylindrotheca* sp., although sediment trap studies indicate that *Pseudo-nitzschia* sp. in particular can sometimes be efficiently exported (Dortch et al. 1997). These dominance shifts could also be ecologically significant, since some *Pseudo-nitzschia* species produce the toxin domoic acid and form harmful blooms.

Our results also suggested that under our experimental conditions chrysophytes have a lower CO_2 requirement compared to coccolithophores and diatoms, since they showed increased abundance at lower pCO_2. In addition to possible direct effects of pCO_2 and temperature, the phytoplankton community structure changes we observed in this experiment are also undoubtedly a function of competition among the different groups under the 4 different experimental regimes.

This change in algal community structure was also associated with the large shifts in microzooplankton species composition and abundance over the course of the experiment, as well as significant differences in grazing pressure by microzooplankton. As described in a companion paper (Rose et al. 2009), large oligotrichous ciliates dominated mainly at high temperature, and small ciliates, at low temperature. In general, throughout most of the experiment, there was an active grazer community capable of consuming much of the daily primary production in all 4 treatments. However, towards the end of the experiment, differences in top-down control by the microzooplankton community may have acted as a positive feedback for the growth of potentially unpalatable coccolithophore species in the greenhouse treatment. Overall, the changes in microzooplankton community structure were likely induced by the changes in phytoplankton community structure rather than by direct effects of CO_2 or temperature on microzooplankton physiology (Rose et al. 2009). Such shifts in multiple trophic levels and their mutual interactions could thus be a feature of future changes in the North Atlantic spring bloom assemblage. It seems clear that warming and rising CO_2 may affect both 'bottom-up' and 'top-down' control mechanisms on the phytoplankton community, and that the net outcome of our manipulative experiments reflects a combination of these 2 inter-related factors (see Rose et al. 2009).

A previous semi-continuous incubation in the tropical Pacific found that a diatom-dominated community developed after CO_2 enrichment to 750 ppm (Tortell et al. 2002), but their study did not explore potential temperature interactions. Hare et al. (2007) reported that originally dominant large diatoms were replaced by smaller nanophytoplankton species after pCO_2 and temperature were both elevated in Bering Sea experiments. Our results also suggest that nanophytoplankton (coccolithophores) may further increase in abundance relative to other phytoplankton groups in the later stages of the future North Atlantic spring bloom if CO_2 concentration and SST continue to increase. Coccolithophores were already the most abundant group in the study area during our cruise, but there were still substantial numbers of diatoms and other algal taxa present too (Leblanc et al. 2009), as has commonly been observed in almost all previous investigations of the bloom (Barlow et al. 1993). Our experiments suggest that changing environmental conditions could result in coccolithophores becoming even more dominant over these other groups in the future than is the case today. This suggestion, arising from our short-term study, will need to be tested by other methods over the coming decades, as the algal community adapts to the same types of changes over longer time scales.

Nutrient and carbon biogeochemistry was influenced by elevated temperature and pCO_2 as well. Concomitant with decreased diatom abundance, the community BSi:POC ratio was significantly decreased by increased temperature. The bulk of total BSi export by the annual bloom probably occurs during the earlier diatom-dominated phase, but, during the late phase in the region we sampled, integrated BSi concentrations were still about 50 % of PIC concentrations, so substantial silica export was likely still underway (Leblanc et al. 2009). Our results suggest lower biogenic silica to particulate carbon export ratios during this part of the bloom in the warmer marine environment of the future.

Although coccolithophore abundance was by far the highest in the greenhouse treatment, the PIC production rate was nevertheless significantly reduced when pCO_2 and temperature were elevated simultaneously. If our experimental results are indicative of longer term trends, they suggest that coccolithophores could be become even more dominant in the late stages of the future North Atlantic spring bloom, while paradoxically calcification could decrease dramatically at the same time.

Riebesell et al. (2000) and Zondervan et al. (2001, 2002) found that CO_2 enrichment alone reduced the calcification of coccolithophores in laboratory incubations. Furthermore, an obvious malformation of coccoliths was observed at pCO_2 of 750 to 880 ppm in 2 coccolithophore species, *Emiliania huxleyi* and

Gephyrocapsa oceanica (Riebesell et al. 2000). In contrast, we found no effect of elevated pCO$_2$ alone on calcification of the North Atlantic natural coccolithophore community. Only when pCO$_2$ was increased in concert with temperature was a significant reduction in the PIC:POC ratio observed. In keeping with this interactive effect of pCO$_2$ with other variables, a laboratory semi-continuous experiment using *E. huxleyi* also found significantly decreased cellular PIC content when pCO$_2$ was elevated to 750 ppm, but only when irradiance was saturating at the same time (Feng et al. 2008). Despite this striking illustration of the importance of other interacting variables, in general, our results are consistent with most literature predicting decreases in calcification in a high CO$_2$ ocean (Riebesell et al. 2000, Feely et al. 2004, Orr et al. 2005). Our results, however, contrast strongly with a recent study that suggested increases in calcification in coccolithophore cultures at high pCO$_2$ (Iglesias-Rodriguez et al. 2008).

It has been hypothesized that bicarbonate (HCO$_3^-$) is the main or only carbon source for calcification, in contrast to the photosynthetic process, in which CO$_2$ is the main carbon source (Paasche 1964, Sikes et al. 1980, Rost & Riebesell 2004). The different responses of calcification and photosynthesis to changes in the marine carbonate system have been recognized as the main causes of decreased PIC/POC (the rain ratio) with increased atmospheric CO$_2$ (Paasche 1964, Riebesell et al. 2000, Berry et al. 2002). Our on-deck incubation was conducted under conditions of complete or near light saturation, as determined by the light saturation value (E_k) from our *P/E* experiments. Nevertheless, decreased calcification was only observed in the greenhouse treatment when both pCO$_2$ and temperature were elevated simultaneously.

In addition to decreased calcification, we also observed large decreases in diatom abundance and the BSi:POC ratio under greenhouse conditions. If these experimental trends are predictive of future responses of the *in situ* community, they suggest significant future reductions in biomineral phases in general during the later part of the bloom. Since organic carbon export is thought to be heavily dependent on 'ballasting' by denser calcite and/or silica (Armstrong et al. 2001, Ziveri et al. 2007), such reductions in algal biomineralization could tend to reduce carbon export by the biological pump during the late North Atlantic spring bloom.

We also recorded the highest DMSP$_p$ concentrations in the greenhouse treatment, accompanying the highest coccolithophore abundance (Lee et al. 2009). Many laboratory and field studies have found that marine haptophytes (including coccolithophores) and dinoflagellates generally have a higher cellular DMSP content than do other groups (Keller et al. 1989, Malin & Steinke 2004). Since DMSP is the major precursor of dimethyl sulfide (DMS), coccolithophore (especially *Emiliania huxleyi*) blooms are well known as high DMS production areas, sometimes with a large contribution from nanoflagellates or dinoflagellates (Steinke et al. 2002, Archer et al. 2003). Increases in DMS production under greenhouse conditions such as those we observed have the potential to increase cloud albedo, and thus be a negative feedback on global warming (Charlson et al. 1987). These results are consistent with the notion that this feedback may accelerate in the future, due to enhanced biomass-specific DMSP production resulting from changes in the North Atlantic spring bloom phytoplankton community in response to increased pCO$_2$ and temperature. A complete discussion of the implications of these changes in the DMSP cycle for climate feedback mechanisms is presented in Lee et al. (2009).

These experimental results provide new evidence indicating that further atmospheric CO$_2$ enrichment coupling with sea surface warming may have additive effects on the phytoplankton community of the North Atlantic spring bloom. We can speculate that under future global change scenarios, marine coccolithophores will be favored more during the late stages of the North Atlantic bloom than will other groups such as diatoms. Biogeochemical consequences may include an increased organic carbon fixation rate, significantly weakened calcification and silicification, and increased DMS production. These hypotheses derived from our short-term experiments will, of course, require further testing using independent methods such as long-term observations and time series. Our experimental simulations of year 2100 pCO$_2$ and temperature demonstrate that both factors exert a proximate control on present day plankton assemblages, and therefore suggest the possibility that future global changes could greatly influence algal productivity, community structure, and carbon, nutrient, and sulfur biogeochemistry in the North Atlantic spring bloom.

LITERATURE CITED

Alley RB, Berntsen T, Bindoff NL, Chen Z and others (2007) Summary for policymakers. In: Solomon S, Qin D, Manning M, Chen Z and others (eds) Climate change 2007:

The physical science basis. Contribution of Working Group I to the fourth assessment report of the Intergovernmental Panel on Climate Change. Cambridge University Press, Cambridge and New York

Archer SD, Stelfox-Widdicombe CE, Malin G, Burkill PH (2003) Is sulphide production related to microzooplankton herbivory in the southern North Sea? J Plankton Res 25: 235–242

Armstrong RA, Lee C, Hedges JI, Honjo S, Wakeham SG (2001) A new, mechanistic model for organic carbon fluxes in the ocean based on the quantitative association of POC with ballast minerals. Deep Sea Res II 49:219–236

Babin M, Morel A, Gagnon R (1994) An incubator designed for extensive and sensitive measurements of phytoplankton photosynthetic parameters. Limnol Oceanogr 39: 496–510

Banse K (1991) Rates of phytoplankton cell division in the field and in iron addition experiments. Limnol Oceanogr 36:1886–1898

Barlow RG, Mantoura RFC, Gough MA, Fileman TW (1993) Pigment signatures of the phytoplankton composition in the northeastern Atlantic during the 1990 spring bloom. Deep Sea Res II 40:459–477

Berry L, Taylor AR, Luken U, Ryan KP, Brownlee C (2002) Calcification and inorganic carbon acquisition in coccolithophores. Aust J Plant Physiol 29:289–299

Bopp L, Mofray P, Aumont O, Dufresne JL and others (2001) Potential impact of climate change on marine export production. Global Biogeochem Cycles 15:81–99

Boyd PW, Doney SC (2002) Modeling regional responses by marine pelagic ecosystems to global climate change. Geophys Res Lett 29, 1806, doi:10.1029/2001GL014130

Bruland KW, Rue EL, Smith GJ, DiTullio GR (2005) Iron, macronutrients and diatom blooms in the Peru upwelling regime: brown and blue waters of Peru. Mar Chem 93: 81–103

Brzezinski MA, Nelson DM (1995) The annual silica cycle in the Sargasso Sea near Bermuda. Deep Sea Res I 42: 1215–1237

Burkhardt S, Riebesell U, Zondervan I (1999) Effects of growth rate, CO_2 concentration, and cell size on the stable carbon isotope fractions in marine phytoplankton. Geochim Cosmochim Acta 63:3729–3741

Burkhardt S, Armoroso G, Ribesell U, Sultemeyer D (2001) CO_2 and HCO_3^- uptake in marine diatoms acclimated to different CO_2 concentrations. Limnol Oceanogr 46: 1378–1391

Charlson RJ, Lovelock JE, Andreae MO, Warren SG (1987) Oceanic phytoplankton, atmospheric sulfur, cloud albedo and climate. Nature 326:655–661

DiTullio GR, Geesey ME (2002) Photosynthetic pigments in marine algae and bacteria. In: Bitton G (ed) The encyclopedia of environmental microbiology. John Wiley & Sons, New York, p 2453–2470

Dortch Q, Robichaux R, Pool S, Milsted D and others (1997) Abundance and vertical flux of *Pseudo-nitzschia* in the northern Gulf of Mexico. Mar Ecol Prog Ser 146:249–264

Eppley RW (1972) Temperature and phytoplankton growth in the sea. Fish Bull 70:1063–1085

Esaias WE, Feldman GC, McClain CR, Elrod JA (1986) Monthly satellite-derived phytoplankton pigment distribution during the spring bloom in the North Atlantic Ocean. Eos Trans AGU 67:835–837

Feely RA, Sabine CL, Lee K, Berelson W, Kleypas J, Fabry VJ, Millero FJ (2004) Impact of anthropogenic CO_2 on the $CaCO_3$ system in the oceans. Science 305:362–366

Feng Y, Warner ME, Zhang Y, Sun J, Rose JM, Fu FX,

Hutchins DA (2008) Interactive effects of increased pCO_2, temperature and irradiance on the marine coccolithophore *Emiliania huxleyi* (Prymnesiophyceae). Eur J Phycol 43: 87–98

Fu FX, Warner ME, Zhang Y, Feng Y, Hutchins DA (2007) Effects of increased temperature and CO_2 on photosynthesis, growth and elemental ratios in marine *Synechococcus* and *Prochlorococcus* (Cyanobacteria). J Phycol 43: 485–496

Gaul W, Antia AN, Koeve W (1999) Microzooplankton grazing and nitrogen supply of phytoplankton growth in the temperate and subtropical northeast Atlantic. Mar Ecol Prog Ser 189:93–104

Geider RJ, Osborne RA (1992) Algal photosynthesis: the measurement of algal gas exchange. Chapman & Hall, New York

Gueguen C, Tortell PD (2008) High resolution measurement of Southern Ocean CO_2 and O_2/Ar by membrane inlet mass spectrometry. Mar Chem 108:184–194

Hare CE, DiTullio GR, Trick CG, Wilhelm SW, Bruland KW, Rue EL, Hutchins DA (2005) Phytoplankton community structure changes following simulated upwelled iron inputs in the Peru upwelling region. Aquat Microb Ecol 38:269–282

Hare CE, Leblanc K, DiTullio GR, Kudela RM and others (2007) Consequences of increased temperature and CO_2 for phytoplankton community structure in the Bering Sea. Mar Ecol Prog Ser 352:9–16

Hays GC, Richardson AJ, Robinson C (2005) Climate change and marine plankton. Trends Ecol Evol 20:337–344

Hobbie JE, Daley RJ, Jasper S (1977) Use of Nuclepore filters for counting bacteria by fluorescent microscopy. Appl Environ Microbiol 33:1225–1228

Hutchins DA, DiTullio GR, Zhang Y, Bruland KW (1998) An iron limitation mosaic in the California coastal upwelling regime. Limnol Oceanogr 43:1037–1054

Hutchins DA, Pustizzi F, Hare CE, DiTullio GR (2003) A shipboard natural community continuous culture system for ecologically relevant low-level nutrient enrichment experiments. Limnol Oceanogr Methods 1:82–91

Hutchins DA, Fu FX, Zhang Y, Warner ME and others (2007) CO_2 concentration controls nitrogen fixation rates of the marine cyanobacterium *Trichodesmium.* Limnol Oceanogr 52:1293–1304

Iglesias-Rodriguez MD, Halloran PR, Rickaby REM, Hall IR and others (2008) Phytoplankton calcification in a high-CO_2 world. Science 320:336–340

Keller MD, Bellows WK, Guillard RRL (1989) Dimethyl sulfide production in marine phytoplankton. In: Saltzman ES, Cooper WJ (eds) Biogenic S in the environment. American Chemical Society, Washington, DC, p 167–182

Leblanc K, Hare CE, Feng Y, Berg GM and others (2009) Distribution of calcifying and silicifying phytoplankton in relation to environmental and biogeochemical parameters during the late stages of the 2005 North East Atlantic spring bloom. Biogeosciences Discussions 6:5789–5847. Available at: www.biogeosciences-discuss.net/6/5789/2009/bgd-6-5789-2009.pdf

Lee PA, Rudisill JR, Neeley AR, Maucher JM and others (2009) Effects of increased pCO_2 and temperature on the North Atlantic spring bloom. III. Dimethylsulfoniopropionate. Mar Ecol Prog Ser 388:41–49

Lochte K, Ducklow HW, Fasham MJR, Stienens C (1993) Plankton succession and carbon cycling at 47° N, 20° W during the JGOFS North Atlantic bloom experiment. Deep Sea Res II 40:91–114

Malin G, Steinke M (2004) Dimethyl sulfide production: What

is the contribution of coccolithophores? In: Thierstein HR, Young JR (eds) Coccolithophores: from molecular processes to global impact. Springer, Heidelberg, p 129–136

Martin-Jezequel V, Hildebrand M, Brzezinski MA (2000) Silicon metabolism in diatoms: implications for growth. J Phycol 36:821–840

Noble RT, Fuhrman JA (1998) Use of SYBR Green I for rapid epifluorescence counts of marine viruses and bacteria. Aquat Microb Ecol 14:113–118

Orr JC, Fabry VJ, Aumont O, Bopp L and others (2005) Anthropogenic ocean acidification over the twenty-first century and its impact on calcifying organisms. Nature 437:681–686

Paasche E (1964) A tracer study of the inorganic carbon uptake during coccolith formation and photosynthesis in the coccolithophorid *Coccolithus huxleyi*. Physiol Plant 3(Suppl):1–82

Paasche E, Brubak S (1994) Enhanced calcification in the coccolithophorid *Emiliania huxleyi* (Haptophyceae) under phosphorus limitation. Phycologia 33:324–330

Passow U, Alldredge AL (1995) A dye-binding assay for the spectrophotometric measurement of transparent exopolymer particles (TEP). Limnol Oceanogr 40:1326–1335

Platt TP, Gallegos CL (1980) Modeling primary production. In: Falkowski PG (eds) Primary productivity in the sea. Plenum Press, New York, p 339–351

Riebesell U (2004) Effects of CO_2 enrichment on marine phytoplankton. J Oceanogr 60:719–729

Riebesell U, Zondervan I, Rost B, Tortell PD, Zeebe RE, Morel FMM (2000) Reduced calcification of marine plankton in response to increased atmospheric CO_2. Nature 407:364–367

Riegman R, Noordeloos AA, Cadee GC (1992) *Phaeocystis* blooms and eutrophication of the continental coastal zones of the North Sea. Mar Biol 112:479–484

Rose JM, Feng Y, Gobler CJ, Gutierrez R, Hare CE, Leblanc K, Hutchins DA (2009) Effects of increased pCO_2 and temperature on the North Atlantic spring bloom. II. Microzooplankton abundance and grazing. Mar Ecol Prog Ser 388:27–40

Rost B, Riebesell U (2004) Coccolithophores and the biological pump: responses to environmental changes. In: Thierstein HR, Young JR (eds) Coccolithophores: from molecular processes to global impact. Springer, New York, p 99–125

Rost B, Riebesell U, Burkhardt S, Sültemeyer D (2003) Carbon acquisition of bloom-forming marine phytoplankton. Limnol Oceanogr 48:55–67

Rousseeuw PJ, van Zomeren BC (1990) Unmasking multivariate outliers and leverage points. J Am Stat Assoc 85:633–639

Sarmiento JL, Hughes TMC, Stouffer RJ, Manabe S (1998) Simulated response of the ocean carbon cycle to anthropogenic climate warming. Nature 393:245–249

Sarmiento JL, Slater R, Barber R, Bopp L and others (2004) Response of ocean ecosystems to climate warming. Global Biogeochem Cycles 18, GB3003, doi: 10.1029/2003GB002134

Sieracki ME, Verity P, Stoecker DK (1993) Plankton community response to sequential silicate and nitrate depletion during the 1989 North Atlantic spring bloom. Deep-Sea Res 40:213–252

Sikes CS, Rober RD, Wilbur KM (1980) Photosynthesis and coccolith formation: inorganic carbon sources and net inorganic reaction of deposition. Limnol Oceanogr 25:248–261

Steinke M, Milan G, Archer SD, Burkill PH, Liss PS (2002) DMS production in a coccolithophorid bloom: evidence for the importance of dinoflagellate DMSP lyases. Aquat Microb Ecol 26:259–270

Tilman D (1977) Resource competition between planktonic algae: an experimental and theoretical approach. Ecology 58:338–348

Tortell PD, DiTullio GR, Sigman DM, Morel FMM (2002) CO_2 effects on taxonomic composition and nutrient utilization in an equatorial Pacific phytoplankton assemblage. Mar Ecol Prog Ser 236:37–43

Tortell PD, Payne CD, Li Y, Trimborn S and others (2008) CO_2 sensitivity of Southern Ocean phytoplankton. Geophys Res Lett 35, L04605, doi:10.1029/2007GL032583

Tyrrell T, Merico A (2004) *Emiliania huxleyi*: bloom observations and the conditions that induce them. In: Thierstein HR, Young JR (eds) Coccolithophores: from molecular processes to global impact. Springer, Heidelberg, p 75–97

Tyrrell T, Taylor AH (1996) A modeling study of *Emiliania huxleyi* in the NE Atlantic. J Mar Syst 9:83–112

Walz PM, Friederich GE (1996) Rapid automated analysis of total dissolved inorganic carbon and its application in the central California upwelling system during the CoOP95 experiment. EOS 76:OS102

Welschmeyer NA (1994) Fluorometric analysis of chlorophyll *a* in the presence of chlorophyll *b* and pheopigments. Limnol Oceanogr 39:1985–1992

Wen K, Ortmann AC, Suttle CA (2004) Accurate estimation of viral abundance by epifluorescence microscopy. Appl Environ Microbiol 70:3862–3867

Wolf-Gladrow DA, Riebesell U, Burkhart S, Bijma J (1999) Direct effects of CO_2 concentration on growth and isotopic composition of marine plankton. Tellus Ser B Chem Phys Meteorol 51:461–476

Zapata M, Rodriguez F, Garrido JL (2000) Separation of chlorophylls and carotenoids from marine phytoplankton: a new HPLC method using a reversed phase C_8 column and pyridine-containing mobile phases. Mar Ecol Prog Ser 195:29–45

Ziveri P, de Bernardi B, Baumann KH, Stoll HM, Mortyn PG (2007) Sinking of coccolith carbonate and potential contribution to organic carbon ballasting in the deep ocean. Deep Sea Res II 54:659–675

Zondervan I, Zeebe RE, Rost B, Rieblesell U (2001) Decreasing marine biogenic calcification: a negative feedback on rising atmospheric pCO_2. Global Biogeochem Cycles 15:507–516

Zondervan I, Rost B, Riebesell U (2002) Effect of CO_2 concentration on the PIC/POC ratio in the coccolithophore *Emiliania huxleyi* grown under light limiting conditions and different day lengths. J Exp Mar Biol Ecol 272:55–70